ORIGINAL ARTICLE

Discovery of a highly potent and orally available importin-β1 inhibitor that overcomes enzalutamide-resistance in advanced prostate cancer

Jia-Luo Huang[a,†], Xue-Long Yan[a,b,†], Dong Huang[a], Lu Gan[a], Huahua Gao[a], Run-Zhu Fan[a], Shen Li[a], Fang-Yu Yuan[a], Xinying Zhu[a], Gui-Hua Tang[a], Hong-Wu Chen[c], Junjian Wang[a,*], Sheng Yin[a,*]

[a]School of Pharmaceutical Sciences, Sun Yat-sen University, Guangzhou 510006, China
[b]School of Pharmacy, Guizhou Medical University, Guian New District, Guizhou 550025, China
[c]School of Medicine, University of California Davis, Sacramento, CA 95817, USA

Abstract Nuclear transporter importin-β1 is emerging as an attractive target by virtue of its prevalence in many cancers. However, the lack of druggable inhibitors restricts its therapeutic proof of concept. In the present work, we optimized a natural importin-β1 inhibitor **DD1** to afford an improved analog **DD1**-Br with better tolerability (>25 folds) and oral bioavailability. **DD1**-Br inhibited the survival of castration-resistant prostate cancer (CRPC) cells with sub-nanomolar potency and completely prevented tumor growth in resistant CRPC models both in monotherapy (0.5 mg/kg) and in enzalutamide-combination therapy. Mechanistic study revealed that by targeting importin-β1, **DD1**-Br markedly inhibited the nuclear accumulation of multiple CRPC drivers, particularly AR-V7, a main contributor to enzalutamide resistance, leading to the integral suppression of downstream oncogenic signaling. This study provides a promising lead for CRPC and demonstrates the potential of overcoming drug resistance in advanced CRPC *via* targeting importin-β1.

---

*Corresponding authors.

E-mail addresses: wangjj87@mail.sysu.edu.cn (Junjian Wang), yinsh2@mail.sysu.edu.cn (Sheng Yin).

[†]These authors made equal contributions to this work.

1. Introduction

Prostate cancer (PC) is the most frequent male cancer and a leading cause of malignancy-related mortality for males[1,2]. Since PC initially depends on androgen for survival and growth, androgen deprivation therapy (ADT) with chemical or surgical castration represents the standard treatment for early-stage PC[3]. However, this disease progresses into a lethal stage known as castration-resistant prostate cancer (CRPC), which could grow under low androgen conditions with restored androgen receptor (AR) signaling[4,5]. Although patients with CRPC could gain certain benefits from AR signaling targeting therapies, such as AR antagonist enzalutamide (ENZ) and androgen synthesis inhibitor abiraterone (ABI), durable responses are limited, largely due to acquired resistance[6,7]. Therefore, the need for novel therapeutics with unique mechanisms to overcome drug resistance in CRPC remains acute.

Karyopherins, known as importins and exportins, are members of nuclear transport receptors involved in the translocation of macromolecules through the nuclear pore complex (NPC)[8–10]. In tumors, specific importins and/or exportins are often overexpressed to meet the extra transportation demand for maintaining the abnormally high rate of cell growth[11,12]. Thus, inhibiting tumor-suppressor proteins being exported out of or oncoproteins being imported into the nucleus *via* regulating karyopherins is considered as a novel approach for cancer therapeutics. With the successful launch of exportin drug, selinexor, a selective inhibitor of exportin-1 (XPO1) to treat multiple myeloma (MM) patients and B-cell lymphoma (BCL) patients, karyopherin members are revealing as appealing therapeutic targets in cancer drug discovery[13,14]. However, the development of importin drugs has been stagnating, owing to the lack of druggable inhibitors for proof-of-concept study.

Importin-β1 (KPNB1) is a key nuclear transporter overexpressed in CRPC[15]. Its expression level is positively correlated with patient's deterioration degree, but the regulatory role remains unclear. In our previous study, we discovered a very potent anti-CRPC agent **DD1** and identified that importin-β1 as the direct target (binding sites: Gln560, Phe577, and Leu580), and further confirmed for the first time that importin-β1 is a druggable vulnerability in CRPC[15]. However, **DD1** had a narrow therapeutic window ($LD_{50} \approx 4$ mg/kg for i.p.) and poor oral bioavailability. Besides, the therapeutic potential of such inhibitors in resistant CRPC still remains unclear. Therefore, an improved analogue with better druggability is in urgent need to clarify the prospect of importin-β1-based CRPC therapy. In the current study, we optimized **DD1** to generate an improved importin-β1 inhibitor **DD1**-Br with better tolerability and oral bioavailability. **DD1**-Br displayed potent anti-CRPC efficacy *in vitro* and *in vivo*, and could overcome the enzalutamide resistance. Mechanistic study showed that by targeting importin-β1, **DD1**-Br significantly inhibited the nuclear accumulation of multiple CRPC drivers, such as AR, E2F1, and MYC, integrally suppressing downstream oncogenic signaling. In particular, the down-regulation of AR-V7 signaling may account for the main mechanism in overcoming enzalutamide resistance. This study opens a new perspective for CRPC drug development, demonstrating the possibility of overcoming drug resistance in advanced prostate cancer *via* importin-β1.

2. Results and discussion

2.1. Structural optimization of *DD1* afforded the improved analogue *DD1*-Br

DD1 is a structurally complex daphnane diterpenoid (DD, 5/7/6 ring system) containing an orthoester functionality. It was selected from a series of active DDs (**DD1**−**DD14**, Fig. 1A) in anti-CRPC screening campaign towards a natural diterpenoid library[15]. As the activity is a major factor prior to other druggability parameters such as toxicity and bioavailability, we firstly tried to obtain the DD analogues with decent anti-CRPC activity. To expand the sample size of this category, simple chemical modifications were conducted on the major isolates **DD1** and **DD4**. As shown in Fig. 1A, the acylation of 5-OH or 20-OH in **DD1** and **DD4** with acetic anhydride or 2-thiophenecarbonyl/benzoyl chlorides afforded a series of acylated derivatives, **DD1a**−**DD1d** and **DD4a**−**DD4d**. Alkaline hydrolysis of **DD4** obtained **DD4e**. As halogenation is known to increase the lipophilicity, membrane permeability, and oral absorption in late-stage lead modification[16], 6,7-epoxy ring was opened by a series halogenides. The ring-opening of 6,7-epoxy in **DD1** with PBr$_3$ afforded 6- or 7-brominated derivatives **DD1**-Br and **DD1g**. The ring-opening of 6,7-epoxy in **DD1** and **DD4** with 36% HCl at room temperature afforded four 6- or 7-chlorinated derivatives **DD1e**, **DD1f**, **DD4f**, and **DD4g**. Besides, the hydrogenation of **DD1** afforded **DD1h** and **DD1i**. Thus, a small library containing 31 natural or synthetic DDs was constructed. The anti-proliferative activity of these DDs on CRPC cell line C4-2B revealed brief structure−activity relationships (SARs): 1) 9,13,14-orthoester group was essential for the activity, as the absence of this functionality resulted in a dramatic decrease of the activity (*e.g.*, **DD11**, **DD12**, and **DD14**); 2) The double bond between C-1 and C-2 is beneficial to the activity (**DD1** *vs* **DD8**). 3) The free OH at C-5 and C-20 was favorable to the activity (**DD4** *vs* **DD4a**−**4d**; **DD1** *vs* **DD1a**−**1d**), while it was unfavorable at C-12 (**DD4** *vs* **DD4e**). 4) The chlorinative and hydroxylated ring-opening of 6,7-epoxy were harmful to the activity (**DD1** *vs* **DD10**, **DD1** *vs* **DD1e** and **DD1f**), but the bromine at C-6 and C-7 restored the activity of the ring-opening products (**DD1**-Br and **DD1g** *vs* **DD10**). The above modifications showed most of the functionalities in **DD1** were untouchable, with only the bromine-substituted analogues **DD1**-Br and **DD1g** and Δ^{15}-hydrogenated analogue **DD1h** maintaining comparable activity to **DD1**. Then, the acute toxicity assay was carried out on these compounds. The results showed that **DD1**-Br had the most improved tolerability ($LD_{50} > 100$ mg/kg for i.p.), being 25-fold greater than that of **DD1** (Fig. 1B and C and Supporting Information Fig. S1A). Furthermore, the pharmacokinetic study also showed that **DD1**-Br had an improved profile in both intraperitoneal (i.p.) and oral (*p.o.*) administrations, with the C_{max} values being 5-fold increase in i.p. and oral bioavailability being 32-fold increase (**DD1**-Br $F = 64.1\%$; **DD1** $F = 2.21\%$, Fig. 1D and Fig. S1B and S1C). Taken together, **DD1**-Br was turned out to be an improved analogue of **DD1** with comparable activity but better druggability.
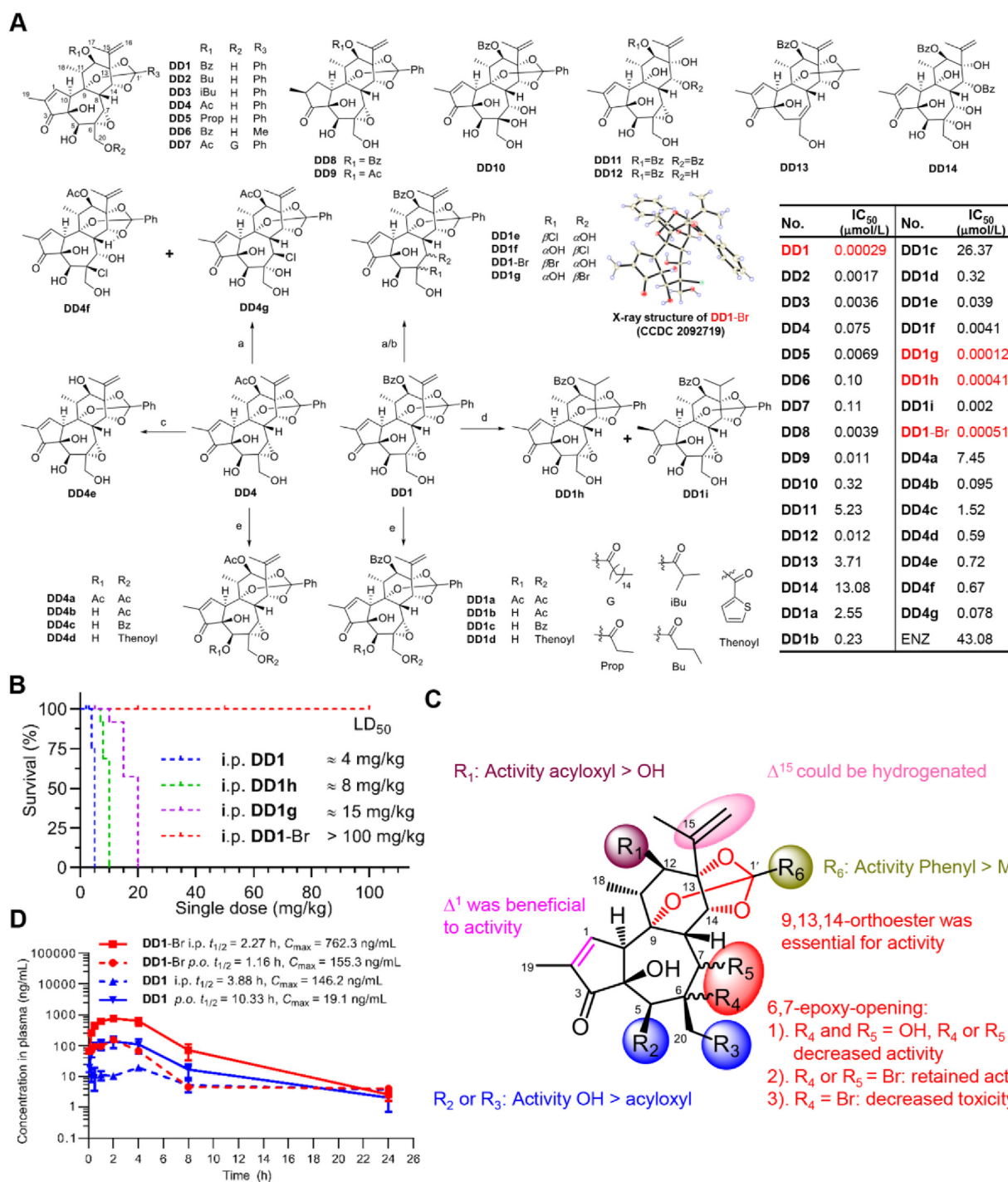
Figure 1 Structural optimization of **DD1** afforded an improved analogue **DD1**-Br with better tolerability and oral bioavailability. (A) Structures of **DD1**−**DD14** and the synthesis of daphnane derivatives. (a) 36% HCl, THF, rt, 0.5 h. (b) PBr$_3$, CH$_2$Cl$_2$, −60 °C. (c) 1% NaOH in MeOH (m/v), rt, 0.5 h. (d) H$_2$, 10% Pd/C, MeOH, 0.5 h. (e) Acetic anhydride/benzoyl chlorides/2-thiophenecarbonyl, Pyr, rt/50 °C. IC$_{50}$s for DDs in C4-2B cells treated for 48 h. (B) Survival curve showing the survival of the mice (KM) after the indicated single dose treatments. The estimated LD$_{50}$ value was indicated. (C) SARs of DDs on anti-proliferative activity and toxicity. (D) ICR mice were treated p.o. or i.p. with 1 mg/kg of **DD1** or **DD1**-Br for pharmacokinetic (PK) analysis. Plasma concentration of **DD1** or **DD1**-Br was measured within 24 h after a single dose treatment. Results are shown as mean ± SD. n = 3 mice at each time point.

2.2. DD1-Br is a potent inhibitor of CRPC cell growth and survival

To systematically evaluate the activity of **DD1**-Br, we tested it on a subset of AR-positive (AR$^+$) CRPC cell lines, AR-negative

(AR$^−$) PC cell lines, and normal cells. The results showed that **DD1**-Br could selectively inhibit the cell growth of AR$^+$ CRPC cell lines (such as C4-2B, VCaP-CRPC, and 22Rv1) at sub-nanomolar range, with SI value being ∼1000 to AR$^−$ cell lines (DU145 and PC-3) and prostatic normal cells (RWPE-1) (Fig. 2A
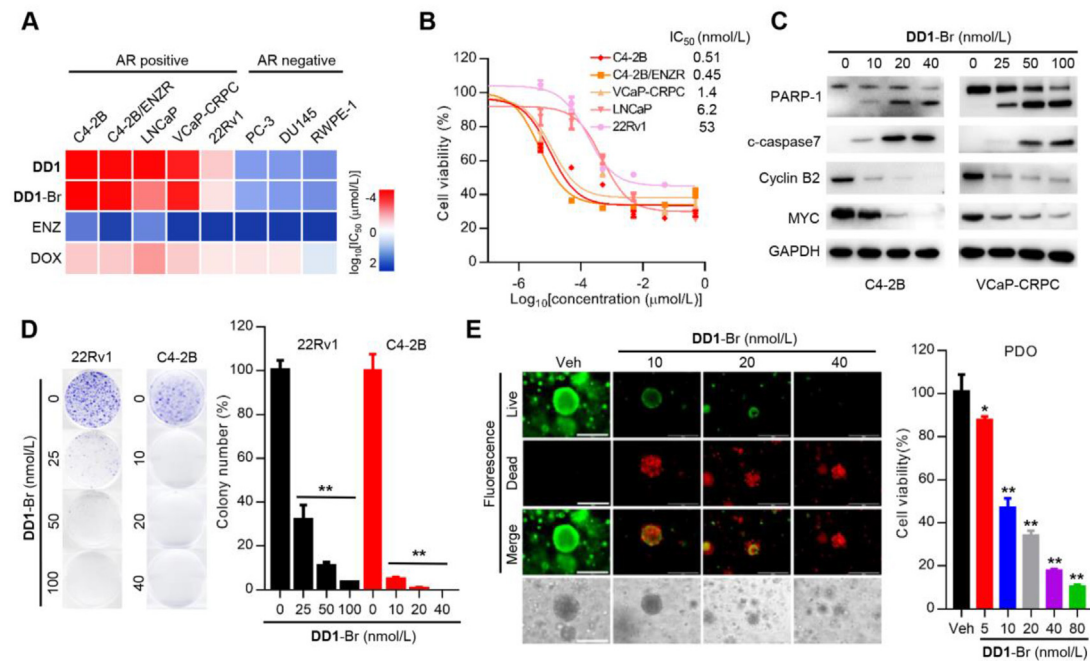
Figure 2 **DD1**-Br significantly inhibits the growth and survival of CRPC cells. (A) IC_{50}s of **DD1**, **DD1**-Br, ENZ, and DOX in AR-positive or AR-negative cell lines treated for 48 h were shown in visual heat map. (B) Dose-dependent inhibition of CRPC cell viability in **DD1**-Br treatment for 48 h. (C) Immunoblotting analysis of **DD1**-Br on expression levels of the designated proteins in C4-2B and VCaP-CRPC cells. Cells were incubated with different concentrations of **DD1**-Br for 24 h. (D) 22Rv1 and C4-2B cells were incubated with different concentrations of **DD1**-Br for 12 days, and then colony formation was assessed. (E) Patient-derived xenograft derived organoids (PDO) were incubated with various concentrations of **DD1**-Br for 6 days. Typical photographs were recorded by microscope and PDO cell viability was assessed. Scale bar = 200 μm. Data in (D) and (E) are presented as mean ± SD. of three independent experiments; *$P < 0.05$, **$P < 0.01$ *vs* control; Student's *t* test.

and B and Supporting Information Fig. S2A). Further studies showed that **DD1**-Br could induce cell apoptosis, as proved by the appearance of the cleaved caspase-7 and poly polymerase 1 (PARP1), and suppress the expression of oncoproteins involved in oncogenesis, survival, and proliferation, such as MYC and cyclin B2 (Fig. 2C and Fig. S2B). Consistent with these effects, **DD1**-Br potently inhibited CRPC cell colony formation (Fig. 2D) and significantly inhibited the growth of the 3D organoid derived from prostate cancer patient-derived xenograft (PDX) (Fig. 2E). Overall, these results indicated that **DD1**-Br could potently inhibit CRPC cell growth and survival.

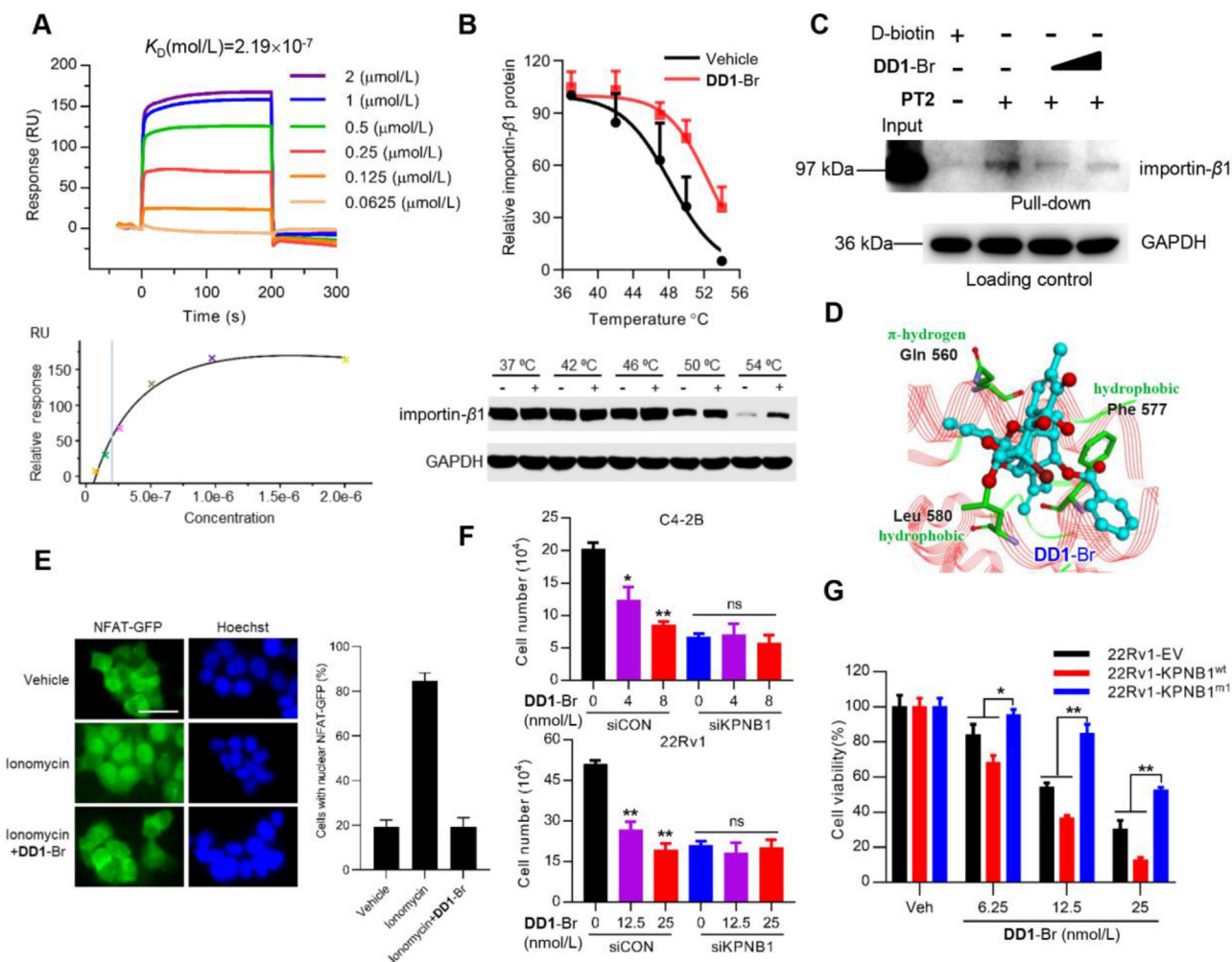### 2.3. DD1-Br targets importin-β1 and its anti-CRPC activity is importin-β1 dependent

To verify if **DD1**-Br still targets importin-β1, the surface plasmon resonance (SPR) experiments and cellular thermal shift assay (CETSA) were performed to investigate the interactions between **DD1**-Br and importin-β1. As shown in Fig. 3A, **DD1**-Br strong bound to importin-β1 (K_D = 0.219 μmol/L, being similar to that of **DD1** (K_D = 0.229 μmol/L)[15], and the ability of **DD1**-Br (20 nmol/L) to enhance the thermostabilization of importin-β1 protein in C4-2B cells indicates target engagement (Fig. 3B). Furthermore, in endogenous affinity pull-down assay, the importin-β1 precipitated by **DD1**-photoaffinity probe (**PT2**)[15] could be competitively offset by **DD1**-Br (Fig. 3C), suggesting that **DD1**-Br shared the same binding modes with **DD1**. This was further confirmed by the high binding affinity between **DD1**-Br and C-terminal 550−876 aa domain of importin-β1 (K_D = 0.201 μmol/L, Fig. S2C) as well as the nice fitting of **DD1**-Br in hydrophobic

pocket formed by the importin-β1 residues Gln560, Phe577, and Leu580 in molecular modeling (Fig. 3D).

Given the known role of importin-β1 in nuclear import, we next investigated the influence of **DD1**-Br on importin-β1-mediated nuclear import in cells by using a reporter system[17]. As shown in Fig. 3E, under the stimulation of calcium ionophore ionomycin, the importin-β1-dependent nuclear accumulation of NFAT-GFP could be significantly decreased by **DD1**-Br, which was consistent with the observed effects of **DD1** and importazole (**IPZ**, a known importin-β1 inhibitor)[15]. We also detected the expression of importin-β1 after **DD1**-Br treatment, and the results showed it had no significant effect (Fig. S2D). Next, we investigated if the anti-proliferative efficacy of **DD1**-Br is dependent on importin-β1. As shown in Fig. 3F, in C4-2B or 22Rv1 cells the knockdown of *KPNB1* significantly attenuated the efficacy of **DD1**-Br as compared to control cells. Importantly, contrary to what was surveyed when expressing KPNB1[wt] in 22Rv1 cells, exogenic expression of KPNB1[m1] (mutation the binding sites Gln560, Phe577, and Leu580) significantly weakened the anti-proliferative effects of **DD1**-Br (Fig. 3G). Collectively, **DD1**-Br exhibited these anti-proliferative effects in CRPC by targeting importin-β1.

2.4. DD1-Br reprograms the nuclear localization of key CRPC survival proteins and shuts down their downstream oncogenic signaling

Given importin-β1 could mediate nuclear import of a cluster of oncoproteins to promote prostate cancer aggressiveness[15,18], we next examined the effect of **DD1**-Br on the nuclear translocation

Figure 3 **DD1**-Br directly targets importin-β1 and its anti-CRPC activity is importin-β1 dependent. (A) Direct interaction between **DD1**-Br and importin-β1 *in vitro* was analyzed by SPR assay. (B) Melt curves of importin-β1 protein in **DD1**-Br (20 nmol/L for 1 h) treated C4-2B cells were measured by CETSA. (C) Endogenous competition assay. 22Rv1 cells were incubated with different concentrations of **DD1**-Br (0, 5 or 10 μmol/L), and meanwhile treated with **PT2** (5 μmol/L) for 6 h. (D) The binding mode of **DD1**-Br and importin-β1 (ID: 2P8Q) according to docking simulation. (E) **DD1**-Br blocks importin-β1-mediated nuclear import in living cells. HEK-293T cells stably expressing NFAT-GFP were treated with **DD1**-Br (40 nmol/L) for 1 h before treatment with ionomycin for 30 min to induce NFAT-GFP nuclear accumulation. Representative images and quantification of the percentage of cells with nuclear NFAT-GFP. Scale bars = 40 μm. (F) Anti-proliferation assay. CRPC cells were transfected with scrambled siCON or *KPNB1* siRNA for 2 days, followed by incubation with different concentrations of **DD1**-Br for 2 days (in C4-2B) or 3 days (in 22Rv1). (G) 22Rv1-EV (empty vector), 22Rv1-KPNB1[wt] and 22Rv1-KPNB1[m1] cells were incubated with various concentrations of **DD1**-Br for 4 day, viable cells were counted. Data in (F) and (G) are represented as mean ± SD. of three independent experiments; *$P < 0.05$, **$P < 0.01$, n.s., not significant *vs* control; Student's *t* test.

of key oncogenic factors in CRPC. As shown in Fig. 4A and B, **DD1**-Br could significantly down-regulated the nuclear accumulation of multiple CRPC drivers, including some transcription factors (*e.g.*, MYC, E2F1, AR, and FOXM1) and coactivators (*e.g.*, PCNA, CREBBP, and PARK7). To further dissect the influence of **DD1**-Br on gene transcription programs, we analyzed RNA-seq transcriptomes of C4-2B cells with the treatment of **DD1**-Br. The results revealed that 4567 genes were markedly down-regulated, while 3916 genes were up-regulated. Among them, the majority of the down-regulated genes were associated with AR, MYC, and E2F pathways using hallmark gene sets analysis, which were subject to the regulation of aforementioned key CRPC transcription factors (Fig. 4C). This was further

corroborated by the gene-set enrichment analysis (GSEA) and RT-PCR verification of target genes (Fig. 4D and E).

Interestingly, RNA-seq analysis revealed that among the **DD1**-Br-affected genes 61.4% were common to those regulated by **DD1** (Fig. 4F). Gene ontology analysis and GSEA suggested that the genes uniquely regulated by **DD1**-Br were associated with biological processes such as cell death, survival, metabolism process, oxygen and migration (Fig. 4G), while those uniquely regulated by **DD1** were related to xenobiotics metabolism, nervous system dysfunction, and dilated cardiomyopathy (Supporting Information Fig. S3A and S3B). These differences may partly explain the improved tolerability and bioavailability of **DD1**-Br as compared with **DD1**.
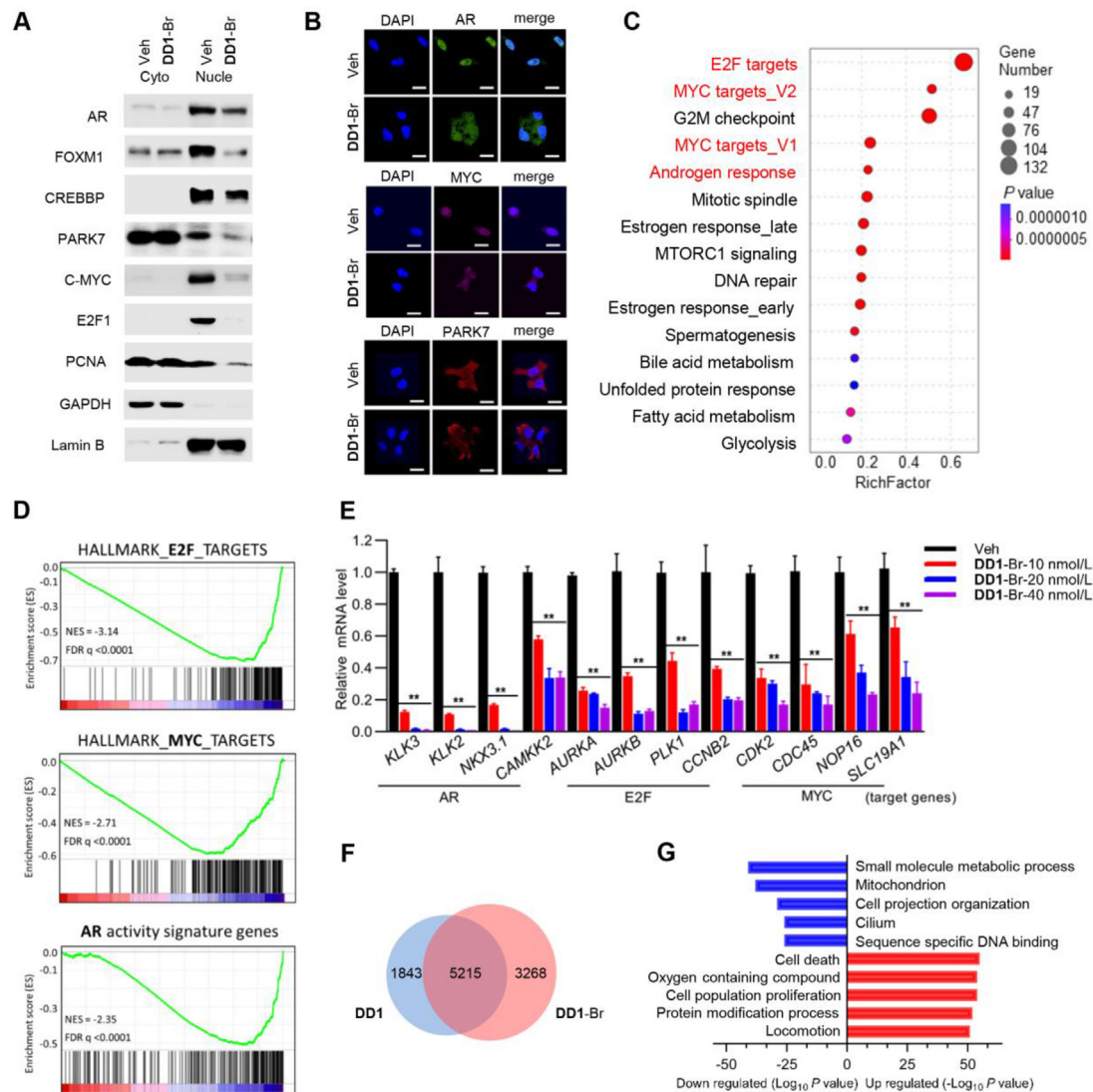
Figure 4 **DD1**-Br alters the key CRPC oncoproteins nuclear accumulation and shuts down their downstream oncogenic signaling. (A, B) Immunoblot and confocal microscopy images detection of the designated proteins in cytoplasm and nucleoplasm in C4-2B cells. Cells were incubated with **DD1**-Br (10 nmol/L) for 6 h. Scale bars = 20 μm. (C) The enrichment analysis of down-regulated genes by **DD1**-Br was displayed by bubble chart. Down-regulated genes were obtained from RNA-seq data of C4-2B cells incubated with **DD1**-Br (20 nmol/L) for 24 h. (D) GSEA profiles for AR, E2F, and MYC pathway signature gene sets from RNA-seq data. (E) qRT-PCR analysis of AR, E2F, and MYC target genes. C4-2B cells were incubated with various concentrations of **DD1**-Br for 24 h. Data are presented as mean ± SD. of three independent experiments; **$P < 0.01$ *vs* control; Student's *t* test. (F and G) Venn diagram (F) showed genes that were regulated by **DD1** (20 nmol/L, 24 h) and **DD1**-Br (20 nmol/L, 24 h) treatment of C4-2B cells from RNA-seq. GO analysis (G) on **DD1**-Br uniquely regulated genes in C4-2B cells.

Taken together, **DD1**-Br could inhibit the nuclear accumulation of vital CRPC survival transcription factors and robustly interrupt their target gene transcription programs.

2.5. *DD1*-Br is a potent, orally available, and tolerable anti-CRPC agent in vivo

Next, we evaluated the efficacy of **DD1**-Br *in vivo* by C4-2B xenograft and PDX models. The results showed that i.p. administration of **DD1**-Br at 0.1 or 0.5 mg/kg markedly inhibited the increase of tumor volume in C4-2B xenografts (Fig. 5A), and i.p.

injected with **DD1**-Br at 0.1 mg/kg could totally prevent the tumor growth in PDX model (Fig. 5B). Immunohistochemical studies supported that the efficacy of **DD1**-Br was paralleled by a decrease of Ki67, an increase of caspase-3, as well as the suppressed nuclear localization of AR, E2F1, MYC, and PARK7 (Fig. 5C and D and Supporting Information Fig. S4A). As the pharmacokinetic profiles of **DD1**-Br showed an improved oral bioavailability, we measured its oral efficacy in 22Rv1 xenograft model for providing data more relevant in a clinical setting. The results indicated that oral dosing of **DD1**-Br at 2 or 0.5 mg/kg still maintained a good efficacy (Fig. 5E).
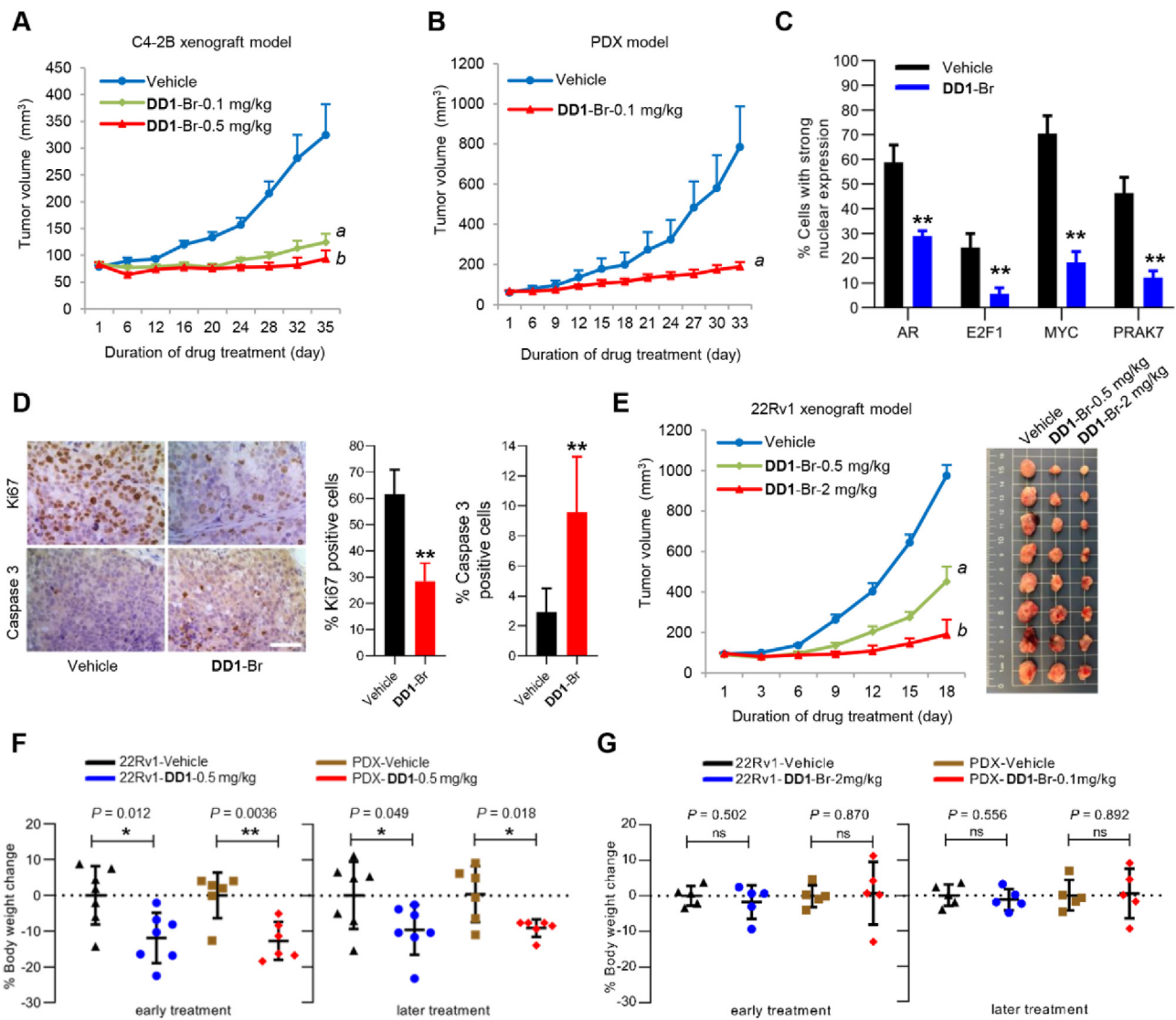
Figure 5 **DD1**-Br is a potent, orally available, and tolerable anti-CRPC agent *in vivo*. (A) Antitumor activity of the designated treatments (**DD1**-Br, 0.5 mg/kg or 0.1 mg/kg, intraperitoneally i.p., 5 times a week, $n = 6$ mice) on the tumor growth of C4-2B xenografts. *a* ($P = 0.0012$); *b* ($P = 0.00044$). (B) Growth curve of PDX model (TM00298) treated with **DD1**-Br (0.1 mg/kg intraperitoneally i.p., 5 times a week, $n = 7$ mice). *a* ($P = 0.013$). (C) IHC quantification of AR, E2F1, MYC, and PARK7 nuclear localization in xenograft tumor tissue of mice bearing PDX treated with vehicle or **DD1**-Br. Data are presented as mean ± SD. **$P < 0.01$ *vs* vehicle; Student's *t* test. (D) Anti-Ki67 or c-caspase 3 IHC images and quantification of tumor section from PDX were shown. Scale bars = 50 μm. (E) Effects of the indicated treatments (**DD1**-Br, oral administrations *p.o.*, daily, $n = 7$ mice) on the growth of 22Rv1 xenografts. *a* ($P = 5.09 \times 10^{-5}$); *b* ($P = 1.63 \times 10^{-8}$). (F) Tolerance test, expressed as percentage change of mice body weight in previous study[15] (on Days 10 and 22 in 22Rv1 tumor models or on Days 15 and 30 in PDX models) for the indicated **DD1** doses. Student's *t* test. (G) Tolerance test, expressed as percentage change of mice body weight in (B) (on Days 15 and 30) and (E) (on Days 9 and 18) for the indicated **DD1**-Br doses. Results in (A), (B), and (E) are presented as the mean tumor volume ± SEM.

In a previous study we found that the treatment of **DD1** (i.p. 0.5 mg/kg, 5 times per week) resulted in mice body weight loss either in the early stage of administration (weight loss ∼13%) or at the end stage of administration (weight loss ∼9%) in both models (Fig. 5F). In contrast, the treatments of **DD1**-Br showed no apparent influence on mice body weight in all administration stages in both 22Rv1 xenograft model and PDX model (Fig. 5G and Fig. S4B). Consistent with this, there were no apparent pathologic abnormalities being observed in the appearance and histological study of multiple organs, including lungs, heart, liver, kidneys, spleen, testicles, and epididymis (Fig. S4C). Additional toxicology analysis further suggested the complete blood count with differential, blood chemistry, and kidney/liver function was normal in **DD1**-Br-treated mice (Fig. S4D). Besides, Discovery Studio software was used to predict and simulate the toxicological properties of **DD1** and **DD1**-Br. As shown in Fig. S4E, consistent with our experimental results, the predicted toxic and side effects of **DD1**-Br were significantly lower than those of **DD1**.

Altogether, these results suggested that **DD1**-Br is an improved analogue of **DD1** with better *in vivo* druggability.

2.6. *DD1-Br inhibited AR-V7 signaling and sensitized resistant CRPC to ENZ*

Enzalutamide (ENZ), the current first-line therapy for CRPC, is encountering the clinical challenge of acquired resistance[19]. Mechanisms of ENZ resistance are rather complex, including intratumoral androgen biosynthesis[20], AR overexpression and amplification[21], AR mutations or generation of AR splicing variants[22,23], as well as activation of parallel pathways[24]. Notably, recent studies have shown that the emergence and continuous activation of AR splicing variants, particularly AR variant 7 (AR-V7), play vital roles in therapeutic resistance[25]. AR-V7 lacks the functional ligand-binding domain (LBD), but remains recruited onto targeted promoters or coactivators to activate oncogene transcription and drive PC progression even in the presence of ENZ[26]. Thus, the suppression of AR-V7 signaling in CRPC may bring the benefits to ENZ therapy.

In protein and RNA-seq analysis, we found that **DD1**-Br could strongly inhibit the nuclear accumulation of AR-V7 and integrally down-regulate its downstream signaling (Fig. 6A−C and Supporting Information Fig. S5A), suggesting that **DD1**-Br may synergize with ENZ in killing resistant CRPC cells. To verify this, the anti-CRPC activity of the combination treatment (**DD1**-Br + ENZ) was evaluated in 22Rv1 and C4-2B/ENZR cells with high AR-V7 expression. As expected, the combination of **DD1**-Br and ENZ in a relatively low concentration synergistically inhibited the colony formations and proliferation of these resistant CRPC cells (Fig. 6D and Fig. S5B and S5C). Moreover, to further demonstrate the synergistic effects were due to the blockage of AR-V7 signaling, we evaluated the coefficient of drug interaction (CDI) of combination therapy after knockdown of AR-V7. As shown in Fig. S5D, **DD1**-Br at 15 nmol/L showed a potent synergistic effect with ENZ in normal 22Rv1 cells (CDI = 0.663), while this synergistic effect was significantly diminished after AR-V7 knockdown (CDI = 1.074), indicating that the inhibition of AR-V7 signaling contributed to the main mechanism of **DD1**-Br + ENZ therapy.

Next, we assessed the *in vivo* combination therapy efficacy in advanced CRPC models. In 22Rv1 xenograft model, administration of **DD1**-Br alone (0.1 mg/kg, i.p.) substantially inhibited the tumor growth, while dosing ENZ alone (10 mg/kg, *p.o.*) did not show significant effect. The combination of these two drugs led to complete growth arrest on tumors, suggesting a potent synergistic effect of the combination therapy (Fig. 6E−G). Moreover, to mimic the human disease more closely, we established a resistant VCaP-CRPC xenograft tumor model based on postcastration relapsed growth of VCaP cells in castrated mice. In this model, the combination of **DD1**-Br (0.5 mg/kg, i.p.) and ENZ (10 mg/kg, *p.o.*) elicited an even more potent synergistic effect, resulting in tumor regression (Fig. 6H, I and Fig. S5E−S5G). Consistent with this, the combination therapy synergistically increased the expression of apoptotic protein cleaved caspase 3 and decreased the expression of proliferative protein Ki67 in tumor tissues of both models (Fig. 6J and Fig. S5H and S5I). It was worth noting that the combination showed no influence on the animal

body weight during the treatment, suggesting its potential safety (Fig. S5J).

Collectively, these results suggested that importin-β1 inhibitor **DD1**-Br could sensitize resistant CRPC tumors to ENZ *via* down-regulating AR-V7 signaling, and **DD1**-Br/ENZ is a promising combination therapy for intractable CRPC.

3. Conclusions

Spurred by the discovery of exportin-1 drug selinexor, importins are emerging as attractive targets in cancer therapies. Several importins, such as importin-β1, importin-α2, and importin-α4, have been demonstrated to be involved in progression in multiple tumors[27−30]. However, the biological function of these importins is mainly investigated by RNA interference (RNAi) methods. The lack of druggable inhibitors hinders their therapeutic potential and further clinical investigation. To the best of our knowledge, only two direct importin inhibitors, importazole and goyazensolide, have been reported before[17,31]. Importazole is a weak importin-β1 inhibitor commonly used as a tool in importin-β1-related study and goyazensolide is a covalent inhibitor of importin-5 showed *in vitro* anti-tumor and anti-viral potentials.

In the current study, we developed a highly potent and orally available importin-β1 inhibitor **DD1**-Br based on previously discovered natural importin-β1 inhibitor **DD1**. With improved tolerability and pharmacokinetic properties, **DD1**-Br displayed remarkable therapeutic efficacy in advanced CRPC xenograft models both in monotherapy and combination therapy. Mechanistic study revealed that by targeting importin-β1, **DD1**-Br significantly blocked the nuclear transport of multiple CRPC drivers, particularly AR-V7, a main contributor to enzalutamide resistance, leading to the integral suppression of downstream oncogenic signaling. This study not only provides an invaluable lead for CRPC treatment, but also demonstrates the possibility of overcoming drug resistance in advanced CRPC *via* targeting importin-β1.

4. Experimental

4.1. *Chemical methods and procedures*

Details of general information, isolation and extraction, plant material, structural elucidation of natural new compounds, synthesis of daphnane derivatives, X-ray crystal structure analysis, and NMR data can be found in the Supporting Information.

4.2. *Biological experiments*

Detailed methods of cell and 3D organoid cultures, cell and 3D organoid viability assays, apoptosis assay, colony formation assay, qPCR, biotin-streptavidin pull-down assay, Western blotting analysis, siRNA transfection, lentivirus preparation, CETSA, confocal immunofluorescence microscopy experiment, molecular docking, expression of recombinant proteins, SPR assay, transcriptome RNA-seq and data analysis, pharmacokinetic studies, acute toxicity experiment, mouse models and treatments,
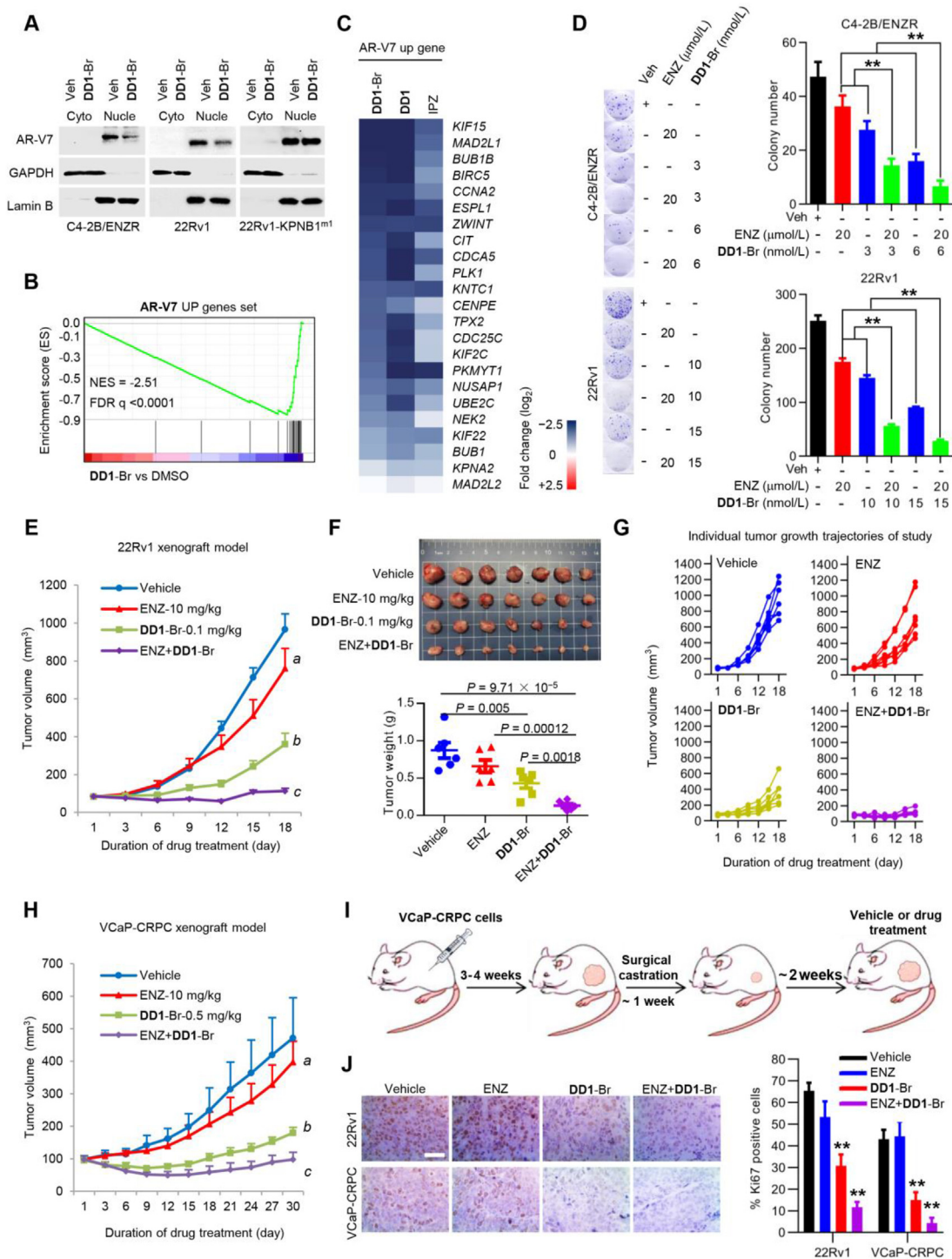
Figure 6 **DD1**-Br inhibited AR-V7 signaling and sensitized resistant CRPC to ENZ. (A) Immunoblotting analysis of AR-V7 in nucleoplasm (Nucle) and cytoplasm (Cyto) of 22Rv1, C4-2B/ENZR, and 22Rv1-KPNB1^{m1} cells treated with **DD1**-Br (10 nmol/L for 6 h in C4-2B/ENZR cells; 25 nmol/L for 24 h in 22Rv1 and 22Rv1-KPNB1^{m1} cells). (B) GSEA of AR-V7 up-regulated genes set in C4-2B cells. Cells were incubated with **DD1**-Br (20 nmol/L) for 24 h. (C) The heatmap presentation of alterations in expression of AR-V7 up-regulated genes in C4-2B cells. Cells were incubated with **DD1**-Br (20 nmol/L), **DD1** (20 nmol/L), or **IPZ** (20 μmol/L) for 24 h. Gene expression was performed by RNA-seq. (D) C4-2B/ENZR and 22Rv1 cells were incubated with designated concentrations of **DD1**-Br, or in combination with ENZ for 14 days. Colony formation images were taken (left), and colony numbers were counted (right), Data are presented as mean ± SD. $n = 3$; **$P < 0.01$ vs control; Student's t test. (E, F) Effects of the indicated treatments (**DD1**-Br, i.p., 0.1 mg/kg; ENZ, p.o., 10 mg/kg; **DD1**-Br and ENZ combined; 5 times a week) on the tumor growth of 22Rv1 xenografts. a ($P = 0.213$, ENZ vs vehicle); b ($P = 9.71 \times 10^{-5}$, **DD1**-Br vs vehicle, $P = 0.0062$, **DD1**-Br vs ENZ); c ($P = 4.32 \times 10^{-7}$, **DD1**-Br + ENZ vs vehicle, $P = 5.74 \times 10^{-5}$, **DD1**-Br + ENZ vs ENZ, $P = 0.0014$, **DD1**-Br + ENZ vs **DD1**-Br) determined by Student's t test at 18 day. Results are presented as the mean tumor volume ± s.e.m. Volumes (left) and weights (right) are shown. (G) Individual

immunohistochemistry, hematology and blood chemistry analysis, and statistics analysis can be found in the Supporting Information.

Acknowledgments

Author contributions

Sheng Yin, and Junjian Wang initiated and supervised the research. Jia-Luo Huang and Xue-Long Yan designed and performed the experiments, interpreted the data, and drafted the manuscript. Lu Gan and Huahua Gao performed partial cellular assays. Dong Huang and Shen Li extracted and purified the tested compounds. Run-Zhu Fan and Xinying Zhu were involved in partial data analysis. Hong-Wu Chen, Fang-Yu Yuan, and Gui-Hua Tang revised the manuscript. All authors read and approved the final manuscript.

Conflicts of interest

The authors declare no conflicts of interest.

Appendix A. Supporting information

Supporting data to this article can be found online at https://doi.org/10.1016/j.apsb.2023.07.017.

References

1. Sung H, Ferlay J, Siegel RL, Laversanne M, Soerjomataram I, Jemal A, et al. Global Cancer Statistics 2020: GLOBOCAN estimates of incidence and mortality worldwide for 36 cancers in 185 countries. *CA Cancer J Clin* 2021;**71**:209−49.
2. Rebello RJ, Oing C, Knudsen KE, Loeb S, Johnson DC, Reiter RE, et al. Prostate cancer. *Nat Rev Dis Prim* 2021;**7**:9.
3. Jacob A, Raj R, Allison DB, Myint ZW. Androgen receptor signaling in prostate cancer and therapeutic strategies. *Cancers* 2021;**13**:5417.
4. Lunardi A, Ala U, Epping MT, Salmena L, Clohessy JG, Webster KA, et al. A co-clinical approach identifies mechanisms and potential therapies for androgen deprivation resistance in prostate cancer. *Nat Genet* 2013;**45**:747−55.
5. Mills IG. Maintaining and reprogramming genomic androgen receptor activity in prostate cancer. *Nat Rev Cancer* 2014;**14**:187−98.
6. Watson PA, Arora VK, Sawyers CL. Emerging mechanisms of resistance to androgen receptor inhibitors in prostate cancer. *Nat Rev Cancer* 2015;**15**:701−11.
7. Wong YN, Ferraldeschi R, Attard G, de Bono J. Evolution of androgen receptor targeted therapy for advanced prostate cancer. *Nat Rev Clin Oncol* 2014;**11**:365−76.
8. Terry LJ, Shows EB, Wente SR. Crossing the nuclear envelope: hierarchical regulation of nucleocytoplasmic transport. *Science* 2007;**318**:1412−6.
9. Cautain B, Hill R, de Pedro N, Link W. Components and regulation of nuclear transport processes. *FEBS J* 2015;**282**:445−62.
10. Tran EJ, Bolger TA, Wente SR. SnapShot: nuclear transport. *Cell* 2007;**131**:420.
11. Mahipal A, Malafa M. Importins and exportins as therapeutic targets in cancer. *Pharmacol Ther* 2016;**164**:135−43.
12. Azmi AS. The evolving role of nuclear transporters in cancer. *Semin Cancer Biol* 2014;**27**:1−2.
13. Azmi AS, Uddin MH, Mohammad RM. The nuclear export protein XPO1—from biology to targeted therapy. *Nat Rev Clin Oncol* 2021;**18**:152−69.
14. Richard S, Richter J, Jagannath S. Selinexor: a first-in-class SINE compound for treatment of relapsed refractory multiple myeloma. *Future Oncol* 2020;**16**:1331−50.
15. Huang JL, Yan XL, Li W, Fan RZ, Li S, Chen J, et al. Discovery of highly potent daphnane diterpenoids uncovers importin-beta1 as a druggable vulnerability in castration-resistant prostate cancer. *J Am Chem Soc* 2022;**144**:17522−32.
16. Gerebtzoff G, Li-Blatter X, Fischer H, Frentzel A, Seelig A. Halogenation of drugs enhances membrane binding and permeation. *Chembiochem* 2004;**5**:676−84.
17. Soderholm JF, Bird SL, Kalab P, Sampathkumar Y, Hasegawa K, Uehara-Bingen M, et al. Importazole, a small molecule inhibitor of the transport receptor importin-beta. *ACS Chem Biol* 2011;**6**:700−8.
18. Rodriguez-Bravo V, Pippa R, Song WM, Carceles-Cordon M, Dominguez-Andres A, Fujiwara N, et al. Nuclear pores promote lethal prostate cancer by increasing POM121-driven E2F1, MYC, and AR nuclear import. *Cell* 2018;**174**:1200−15.
19. Buttigliero C, Tucci M, Bertaglia V, Vignani F, Bironzo P, Di Maio M, et al. Understanding and overcoming the mechanisms of primary and acquired resistance to abiraterone and enzalutamide in castration resistant prostate cancer. *Cancer Treat Rev* 2015;**41**:884−92.
20. Liu C, Lou W, Zhu Y, Yang JC, Nadiminty N, Gaikwad NW, et al. Intracrine androgens and AKR1C3 activation confer resistance to enzalutamide in prostate cancer. *Cancer Res* 2015;**75**:1413−22.
21. Visakorpi T, Hyytinen E, Koivisto P, Tanner M, Keinanen R, Palmberg C, et al. *In vivo* amplification of the androgen receptor gene and progression of human prostate cancer. *Nat Genet* 1995;**9**:401−6.
22. Grasso CS, Wu YM, Robinson DR, Cao X, Dhanasekaran SM, Khan AP, et al. The mutational landscape of lethal castration-resistant prostate cancer. *Nature* 2012;**487**:239−43.
23. Nakazawa M, Antonarakis ES, Luo J. Androgen receptor splice variants in the era of enzalutamide and abiraterone. *Horm Cancer* 2014;**5**:265−73.
24. Arora VK, Schenkein E, Murali R, Subudhi SK, Wongvipat J, Balbas MD, et al. Glucocorticoid receptor confers resistance to antiandrogens by bypassing androgen receptor blockade. *Cell* 2013;**155**:1309−22.
25. Antonarakis ES, Lu C, Wang H, Luber B, Nakazawa M, Roeser JC, et al. AR-V7 and resistance to enzalutamide and abiraterone in prostate cancer. *N Engl J Med* 2014;**371**:1028−38.
26. Li Y, Chan SC, Brand LJ, Hwang TH, Silverstein KA, Dehm SM. Androgen receptor splice variants mediate enzalutamide resistance in

tumor growth trajectories in (E). (H) Effects of the indicated treatments (**DD1**-Br, i.p., 0.5 mg/kg; ENZ, *p.o.*, 10 mg/kg; **DD1**-Br and ENZ combined; 5 times a week) on the tumor growth of VCaP-CRPC xenografts in castrated mice. a ($P = 0.497$, ENZ *vs* vehicle); b ($P = 0.037$, **DD1**-Br *vs* vehicle, $P = 0.012$, **DD1**-Br *vs* ENZ); c ($P = 0.013$, **DD1**-Br + ENZ *vs* vehicle, $P = 0.0021$, **DD1**-Br + ENZ *vs* ENZ, $P = 0.021$, **DD1**-Br + ENZ *vs* **DD1**-Br) determined by Student's t test at 30 day. (I) Establishment and treatment of VCaP-CRPC xenograft model. (J) Anti-Ki67 IHC images and quantification of tumor cells from (E) and (H). Scale bars = 50 μm.

castration-resistant prostate cancer cell lines. *Cancer Res* 2013;**73**: 483−9.

27. Kodama M, Kodama T, Newberg JY, Katayama H, Kobayashi M, Hanash SM, et al. *In vivo* loss-of-function screens identify KPNB1 as a new druggable oncogene in epithelial ovarian cancer. *Proc Natl Acad Sci U S A* 2017;**114**:E7301−10.

28. Du W, Zhu J, Zeng Y, Liu T, Zhang Y, Cai T, et al. KPNB1-mediated nuclear translocation of PD-L1 promotes non-small cell lung cancer cell proliferation *via* the Gas6/MerTK signaling pathway. *Cell Death Differ* 2021;**28**:1284−300.

29. Christiansen A, Dyrskjot L. The functional role of the novel biomarker karyopherin alpha 2 (KPNA2) in cancer. *Cancer Lett* 2013;**331**:18−23.

30. Hazawa M, Sakai K, Kobayashi A, Yoshino H, Iga Y, Iwashima Y, et al. Disease-specific alteration of karyopherin-alpha subtype establishes feed-forward oncogenic signaling in head and neck squamous cell carcinoma. *Oncogene* 2020;**39**:2212−23.

31. Liu W, Patouret R, Barluenga S, Plank M, Loewith R, Winssinger N. Identification of a covalent importin-5 inhibitor, Goyazensolide, from a collective synthesis of Furanoheliangolides. *ACS Cent Sci* 2021;**7**: 954−62.